Supplementary Material (ESI) for Chemical Communications

DNA-Capped Nanoparticles Designed for Doxorubicin Drug Delivery

Colleen M. Alexander, Mathew M. Maye* and James C. Dabrowiak*

Department of Chemistry, Syracuse University, Syracuse New York, 13244 U.S.A.
*mmmaye@syr.edu; *jcdabrow@syr.edu

Supporting Information

Experimental Details

All materials, unless otherwise specified, were purchased from Sigma Aldrich. All oligonucleotides, including **1a/2a** precursors, **1b/2b**, and **1b/2b**-CY3 (excluding CT-DNA) were purchased from Integrated DNA Technologies.

Experimental Design

Nanoparticle Synthesis and DNA-functionalization (1a/2a-AuNP): The gold nanoparticles (AuNP) with average diameters of 15.5 ± 3.1 nm AuNPs were synthesized by standard citrate reduction method (S1-S2). Next, the AuNP were functionalized with ssDNA using methods for high DNA coverage (S3). Briefly, the **1a** and **2a** were purchased as disulfides, and first reduced using dithiothrietol, to produce **1a**/**2a** (containing a 5'-terminal thiol), which were then purified using a Sephadex G-25 column. Next, the AuNP were incubated with **1a** or **2a** at 300x molar ratio ([**1a**]/[AuNP]), and then subjected to the salt aging process (S1, S3). The [**1a**] and [**2a**] stock concentrations were determined using UV-visible spectroscopy (UV-vis), based on extinction coefficients, ε_{260} = 304,800 and 316,900 $M^{-1}cm^{-1}$, respectively. The [AuNP] was similarly determined based on $\varepsilon_{525} = 2 \times 10^8$ $M^{-1}cm^{-1}$.

The **1a**-AuNP or **2a**-AuNP were then purified via centrifugation. The average DNA loading on each AuNP (~33 ± 2) was estimated for **1a**-AuNP based on measurement of DNA uptake, as measured during purification. The number of **1ab** and **2ab** molecules per AuNP was later confirmed using fluorescence spectroscopy (S3), see below.

DNA-Hybridization (1ab/2ab-AuNP): In a typical hybridization experiment, **1a- or 2a**-AuNP was combined with 100 molar excess of the respective partial complement **1b**, or **2b,** forming **1ab** or **2ab** dsDNA functionalized AuNP (**1ab-AuNP**, **2ab-AuNP**). To promote full hybridization, the solution was heated to 60 ^oC, and allowed to cool to room temperature for 1 h, and then remain at room temperature for an additional 1 h. The **1ab- or 2ab**-AuNP were then purified of free **1b** or **2b** via centrifugation. All final **1ab- or 2ab**-AuNP was resuspended in PBS (100 mM NaCl, 10 mM phosphate buffer, pH=7.4). Washing/resuspension was repeated at least three times.

To determine the average loading of **1ab** and **2ab** on AuNP, we employed fluorescence spectroscopy using a dye-modified **1b**/**2b** ssDNA. Briefly, we utilized samples of **1a/2a**-AuNP with **1b/2b**-CY3 (**1b/2b** modified by covalent attachment of the fluorescent dye, CY3) as described above, except that **1a/2b**-AuNP was combined with a specified molar excess of **1b/2b**-CY3. Following hybridization, each solution was centrifuged, removing the **1ab/2ab-Cy3-**AuNP, and the supernatant containing excess **1b/2b**-CY3 was removed and compared to a concentration calibration curve prepared for **1b/2b-CY3**. Each experiment was performed in triplicate. Using this method (S3), we calculated an average number of 36 ± 1 **1ab** dsDNA and 27 ± 1 **2ab** dsDNA at each AuNP. Based on the loading of the high affinity sequence, we then were able to calculate the appropriate number of DOX drugs to add to a known concentration of AuNP, as described next.

* *Department of Chemistry, Syracuse University, 111 College Pl., Syracuse, NY 13244-4100. E-mail: mmmaye@syr.edu; jcdabrow@syr.edu*
† Electronic Supplementary Information (ESI) available: Experimental design and Figures S1-S5. See DOI: 10.1039/b000000x/

Drug Loading and Thermal Denaturation Analysis: We next utilized the **1ab**- or **2ab**-AuNP prepared above, with dsDNA-functionalization, for drug (DOX) loading. For each DOX binding and melting experiment, **1ab**- or **2ab**-AuNP were incubated for 40 min with DOX at specific ratios, r = [DOX]/[**1ab**/**2ab**]. In this study, we explored r = 0 - 12, based on the number of **1ab** per AuNP, as well as the number of binding sites at each **1ab**. Next, each DOX-**1ab**-AuNP was analyzed via thermal denaturation melting experiments using temperature controlled UV-vis at Abs = 260 nm and a heating rate of 1 ^{o}C/min from 25 ^{o}C to 80 ^{o}C. Each melting temperature was taken as the maximum of a peak-fitted first derivative plot of its corresponding melting curve (using PeakFit® Peak Separation and Analysis Software, V.4.12). The [DOX] was calculated for DOX stock solutions based on ε_{480} = 11,500 $M^{-1}cm^{-1}$(S4).

Drug Release: To monitor the release of DOX bound to the **1ab**-AuNP, we employed a transfer dialysis experiment. Briefly, a concentrated solution ([AuNP] = 197.3 nM) of DOX-**1ab**-AuNP (r = 1) was placed inside a dialysis membrane (Spectra/Por Biotech regenerated cellulose dialysis membrane, MWCO = 15kD), and the loaded membrane was placed in a 8.53 x 10^{-4} M solution of duplex calf thymus DNA (CT-DNA) in PBS (10 mM phosphate buffer, 100 mM NaCl, pH = 7.4) and stirred for 24 h. After this time, a UV-vis spectral analysis of the solution containing CT-DNA showed the characteristic spectrum of DOX bound to DNA. Using, ε_{505} = 6,930 $M^{-1}cm^{-1}$, (S4), the [DOX] in the solution containing CT-DNA was calculated and the percentage of particle-bound drug transferred to the CT-DNA outside the membrane was determined to be 27.5%. Two controls, which only deviated from the experimental conditions by the contents of the dialysis membrane, were carried out. A control containing only **1ab**-AuNP in the dialysis membrane verified that no AuNP passed through the membrane, and a second control containing only DOX in the dialysis membrane verified that DOX passes through the membrane and binds CT-DNA to produce the spectrum noted in the drug transfer experiment.

Instrumentation

UV-visible Absorption (UV-vis): The UV-vis measurements were collected on a Varian Cary100 Bio UV-vis spectrophotometer between 200-900nm. The instrument is equipped with an 8-cell automated holder with high precision Peltier heating controller.

Dynamic Light Scattering (DLS): Dynamic Light Scattering (DLS) measurements were collected using a Malvern Zetasizer ZS instrument equipped with a 633 nm laser source, and a backscattering detector at 173^{o}. Each D_h value reported is an average of multiple measurements (3-4), in which each measurement consisted of 11 data collection runs. The average instrumental error on D_h was 1.7 nm.

Fluorescence Spectroscopy: The PL emission and excitation measurements were collected on a Fluoromax-4 photon counting spectrofluorometer (Horiba Jobin Yvon). The instrument is equipped with a 150W xenon white light excitation source and computer controlled monochromator. The detector is a R928P high sensitivity photon counting detector that is calibrated to emission wavelength. All PL emission and excitation spectra were collected using both wavelength correction of source intensity and detector sensitivity. The instrument is equipped with a computer-controlled temperature controller provided by a Thermo NESLAB temperature recirculator (Thermo Scientific).

Transmission Electron Microscopy (TEM): TEM measurements were performed on either a FEI T12 Twin TEM operated at 120 kV with a LaB6 filament and Gatan Orius dual-scan CCD camera (Cornell Center for Materials Research), or a JEOL 2000EX instrument operated at 120 kV with a tungsten filament (SUNY-ESF, N.C. Brown Center for Ultrastructure Studies). Particle size was analyzed manually by modeling each AuNP as a sphere, with statistical analsysis performed using ImageJ software on populations of at least 100 counts.

Supporting Tables/Figures

Table S1. Thermal denaturation temperature, T_m, SPR wavelength, λ_{SPR}, and hydrodynamic diameter, D_h, of **1ab**/**2ab**-AuNP with [DOX]/[**1ab**/**2ab**] = r = 0-12

r	**1ab**-AuNP				**2ab**-AuNP		
	T_m' (ºC)	T_m'' (ºC)	λ_{SPR} (nm)	D_h (nm)	T_m'' (ºC)	λ_{SPR} (nm)	D_h (nm)
0.0		56.6	527	30.9	58.0	525	27.5
1.5		58.9	527	32.1			
3.0*	28	59.9	527	32.9	60.7	525	27.0
4.5	28	62.1	528	34.1			
6.0	29	63.8	537	34.5	61.9	525	26.9
7.5	30	64.9	542	34.7			
9.0	33	63.9	542	34.4	62.2	525	27.0
10.5	30	64.7	545	34.2			
12	35	65.4	547	34.6	62.9	525	27.1

*r = 3.0 values for **1ab**-AuNP are averages of triplicate samples (T_m' = 28±2 ºC, and T_m'' = 59.9±0.8 ºC). Note that T_m' refers to the low T_m feature, and T_m'' refers to the DNA T_m observed for **1ab**-AuNP.

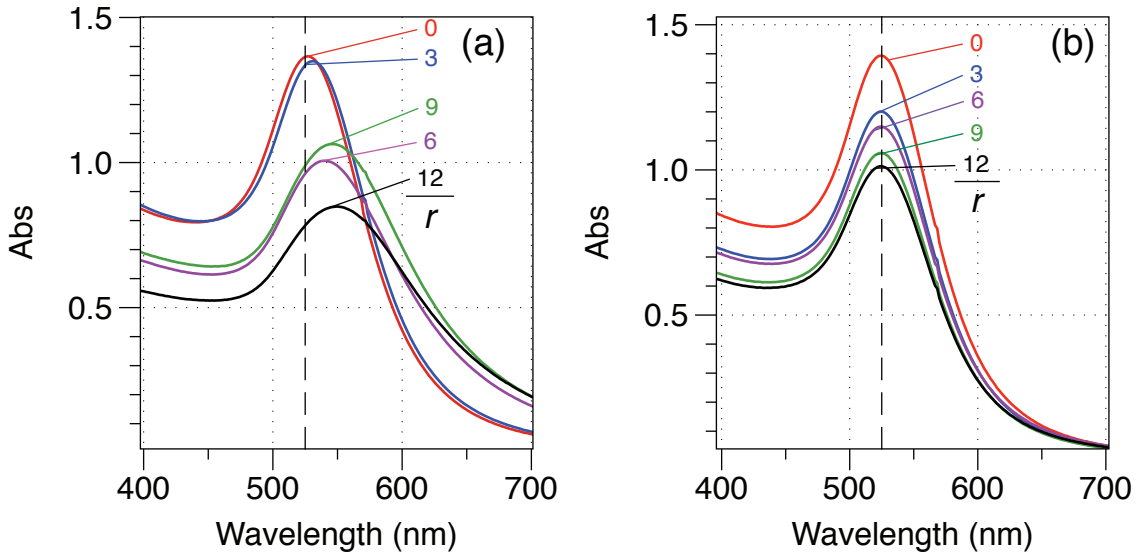

Figure S1. Representative UV-vis spectra for **1ab**-AuNP (a) and **2ab**-AuNP (b) at DOX loadings of r = [DOX]/[**1ab**/**2ab**] = 0, 3, 6, 9, 12. ([AuNP]=14nM, 10 mM phosphate buffer, 100mM NaCl, pH= 7.4).

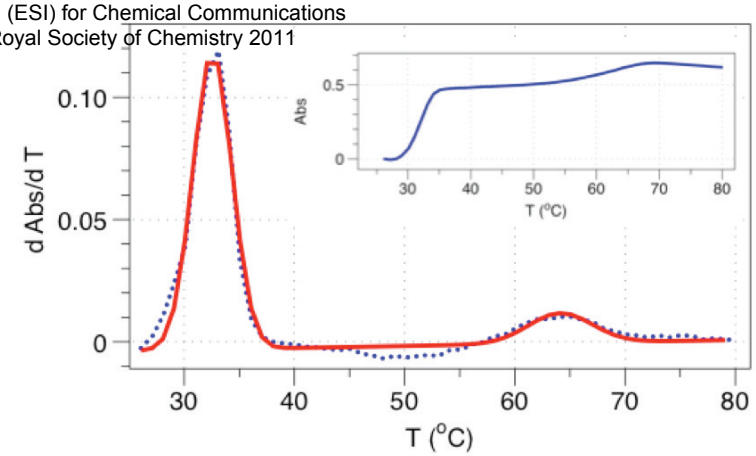

Figure S2. A representative first derivative plot of thermal denaturation of DOX-**1ab**-AuNP at r = 9. Inset: The corresponding thermal denaturation profile. (1 °C/min, 10 mM phosphate buffer, 100mM NaCl, pH= 7.4).

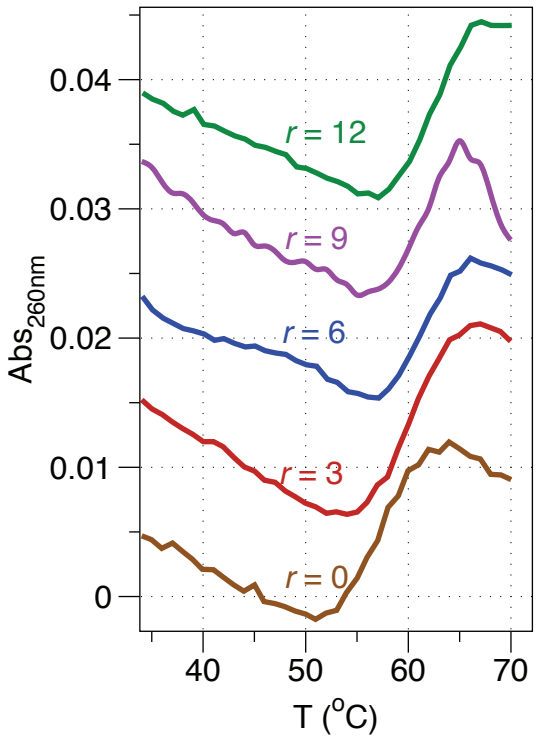

Figure S3. The Thermal denaturation plots for **2ab**-AuNP at r = [DOX]/[**1ab**] = 0, 3, 6, 9, 12. r = 0 – 12. Melting profiles have been normalized and off-set for clarity. (1 °C/min, 10 mM phosphate buffer, 100mM NaCl, pH= 7.4).

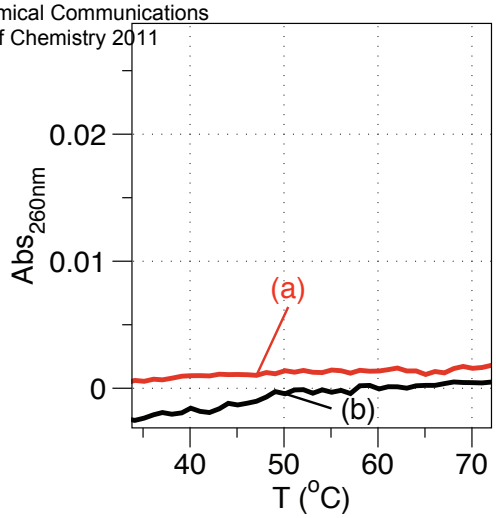

Figure S4. Thermal denaturation control studies for DOX (a, *r* = 12, [DOX] = 5.9 μM) and DOX-**1a**-AuNP (b, *r* = 12; [AuNP] = 13.7 nM. Cooperative melting in the temperature range of ~55-65 °C is not observed for either control.

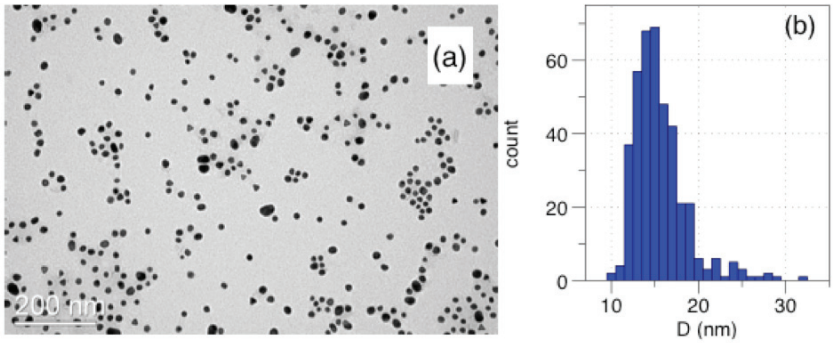

Figure S5. Representative TEM micrograph (a) and statistical analysis (b) for **1a**-AuNP with diameter of 15.5 ± 3.1 nm (*n*=399).

Supporting References:

S1: Maye, M.M.; Nykypanchuk, D.; Van der Lelie, D.; Gang, O. *J. Am. Chem. Soc.* **2006**, 128, 14020-14021.
S2: Freeman, R. G.; Hommer, M. B.; Grabar, K. C.; Jackson, M. A.; Natan, M. J. *J. Phys. Chem*. **1996**, *100*, 718-724.
S3: (a) A. K. R. Lytton-Jean, C. A. Mirkin, *J. Am. Chem. Soc.* **127**, (2005) 12754. (b) Demers, L.M.; Mirkin, C.A.; Mucic, R.C.; Reynolds, R.A.; Letsinger, R.L.; Elghanian, R.; Viswanadham, G. *Anal. Chem.* 2000, **72**, 5535. (c) S. J. Hurst, A. K. R. Lytton-Jean, C. A. Mirkin, *Anal. Chem.*, **78**, 8313 (2006).
S4: Gabbay, E.J.; Grier, D.; Fingerle, R.E.; Riemer, R.; Levy, R.; Pearce, S.W.; Wilson, W.D. *Biochemistry* **1976**, 15, 2062-2070.